INFLUENCE OF THE SPEED OF PLASMA-ARC WELDING AT A VARIABLE POLARITY ASYMMETRICAL CURRENT ON THE FORMATION OF JOINTS OF HIGH-STRENGTH ALUMINIUM ALLOYS

V.M. Korzhyk[1], A.A. Grynyuk[1], V.Yu. Khaskin[1], E.V. Illyashenko[1], S.I. Peleshenko[2], A.O. Aloshyn[2], I.O. Skachkov[3], O.V. Dolyanivska[3]

[1]E.O. Paton Electric Welding Institute of the NASU
11 Kazymyr Malevych Str., 03150, Kyiv, Ukraine
[2]LLC "Foreign Economic Representation of the E.O. Paton Chinese-Ukrainian Institute of Welding
11 Kazymyr Malevych Str., 03150, Kyiv, Ukraine
[3]National Technical University of Ukraine "Igor Sikorsky Kyiv Polytechnic Institute"
37 Peremohy Prosp., 03056, Kyiv, Ukraine

ABSTRACT

The effect of change in the speed of movement of the heating source in plasma-arc welding of aluminium alloys of 2.0 mm thick of three Al–Mg–Mn (AMg5M, AMg6), Al–Cu–Mn (1201) and Al–Cu–Li (1460) alloying systems on the microstructure and hardness of the weld metal and near-weld zone, on the formation of inner pores and mechanical properties of welded joints was considered. Changes in the distribution of temperature fields and indices of the stress-strain state of welded specimens were analyzed. It was found that for each type of alloys there is a certain "peak" welding speed, with exceeding of which there is no significant reduction in residual deformations and stresses, as well as a decrease in the width of the base metal heating zone. Instead, mechanical properties of welded joints are deteriorated because of an increase in the number of pores in the weld metal and the formation of inadmissible undercuts in the upper part of the weld in the area of transition from the weld to the base metal. On the example of Al–Mg–Mn alloy it is shown that such regularities are also typical not only for the thickness of 2.0 mm, but also observed during welding of specimens with the range of thicknesses of 4–8 mm. This allows using these results to predict indices of strength of the welded joint and weld metal for these thicknesses when the speed of plasma-arc welding at a variable polarity asymmetrical current is increased higher than the "peak" value.

KEYWORDS: plasma-arc welding, variable polarity pulses, aluminium alloys, weld structure, pores, joint formation, strength, temperature distribution, stress-strain state

INTRODUCTION

Structures manufactured of high-strength aluminium alloys are used in many fields of the modern industry, namely in the aerospace industry and in ground and water transport production [1]. In order to reduce the total weight of such structures, it is rational to use high-strength aluminium alloys (e.g., Al–Mg–Mn, Al–Cu–Mn and Al–Cu–Li). Aluminium alloys of alloying systems Al–Cu–Mn and Al–Cu–Li have high indices of specific strength, but these alloys are sensitive to excessive heating during welding. This causes a need in creating welding technologies to reduce the heat input into the base metal during welding, including due to the use of higher welding speeds. Traditionally, the joints of parts of Al–Cu–Mn and Al–Cu–Li alloys were produced with the help of a well-known process of argon tungsten-arc welding (TIG) at a variable polarity current [2]. This process is characterized by a low concentration of power in the heating spot. Here, wide and shallow welds are formed. Such low penetration capacity of the heating source in argon tungsten arc welding at a variable polarity current

necessitates the edge preparation in welding parts of more than 4 mm thickness. The heat released during TIG welding at a low power concentration in the heating spot causes softening of high-strength aluminium alloys in the heat-affected zone (HAZ) under the effect of arc heat [3]. In addition, aluminium alloys with the lithium content are prone to the formation of defects in the form of oxide inclusions in the process of argon-arc welding. To solve this problem, it is rational to use welding methods providing an increase in the concentration of power in the heating spot and allow increasing the welding speed, reducing the heat input into the base metal due to these factors, that will allow reducing the level of softening of the base metal in the HAZ of the heating source and improving the mechanical properties of welded joints.

Despite that the process of plasma-arc welding at a variable polarity asymmetrical current exists many years at the market (the first publications date back to the mid-1980s), this method of welding is relevant and in demand nowadays thanks to the use of welding sources on the basis of inverter technology of current conversion and a widespread use of welding robots [4–7].

ANALYSIS OF LITERATURE DATA AND PROBLEM STATEMENT

It is rational to use plasma-arc welding at a variable polarity asymmetrical current for the formation of high-strength aluminium alloys welded joints, which provides a power density of at least 300 W/mm^2, which is 5 times higher than this index compared to TIG, as well as up to 3 times increase in the speed of welding for parts of certain thicknesses [8]. Welding speed is one of the important factors to increase the efficiency of producing welded joint. At the same time, with an increase in the welding speed, an increase in the indices of strength of welded joints, as well as reducing the deformation of the structure during welding are observed. Despite the advantages of welding at high speeds, it is required to use more powerful power sources of welding current, plasmatrons with a more complex design and more complex and more accurate mechanisms for movement of plasmatrons. A logical question arises concerning the limit to which welding speed can be increased and whether there is such a limit in the welding speed, on reaching which, there is no longer a significant decrease in the level of deformation of a structure and a significant increase in strength indices. As the criteria for evaluating such welding speed, it is necessary to consider a significant decrease in the increment of strength indices, negative changes in the formation of welded joint geometry and arising of probable defects in the weld metal. It is rational to consider this issue both from the standpoint of the influence of speed on the formation of macrogeometry and microstructures of the weld, and from the standpoint of its influence on the residual stress-strain state of the structure.

The effect of plasma-arc welding speed on the produced joints from different materials was studied to some degree by various researchers. For example, such data were obtained by optimizing the process of plasma-arc welding (PAW) of duplex stainless 2205 steel of 2 mm thickness [9]. The parameters considered for experimentation and optimization include welding current, welding speed and length of the pilot arc, respectively. The experiment included the change in parameters and further registration of penetration depth and weld width. Welding current of 60–70 A, welding speed of 25.0–30.0 cm/min and pilot arc length of 1–2 mm is a range, in which the mode parameters were changed. During the experiments, a neural network with feedback was used. A genetic algorithm and Taguchi methods were used to predict the width and penetration depth. It was determined that the calculated forecasts are well confirmed by experimentally achieved results, and welding on optimized parametric values provides an increase in the strength of the weld with a reduction in consumables and time.

In [10] the issue of the effect of plasma-arc welding speed in the mode of a keyhole formation (K-PAW) on the quality of penetration and hot cracks formation in welding of the hastelloy X alloy was studied. K-PAW welding was carried out in one pass at speeds of 21.0, 19.0, 17.0 and 15.0 cm/min. Welding at a speed of 170 mm/min provided the best depth to width ratio in the weld compared to all other speeds, and hot cracks were detected at 15.0 cm/min due to a high heat input at a low speed. At welding speeds of 21.0 and 19.0 cm/min, insufficient penetration depth was detected as a result of a reduction in the heat input and the lack of keyhole penetration on the back side. The maximum Vickers microhardness was observed at a welding speed of 21.0 cm/min, and the lowest one at 15.0 cm/min, i.e. the value of the microhardness is inversely proportional to the welding speed. The speed of 170 mm/min provided the best welding quality in view of the depth/width ratio and almost the highest value of microhardness.

The comparison of plasma welding with conventional TIG welding showed [11] that in the case of using plasma process, it is possible to increase the welding speed, which causes an increase in the strength of joints during rupture tests, an increase in ductility indices, reduction of dendrites sizes, HAZ sizes and residual deformations. However, researchers in [12] have found that with a significant increase in welding speed (up to 150–200 cm/min), a constricted arc begins to burn unstable, and at even greater increase in welding speed, even the weld formation is stopped.

However, there were no comprehensive studies on determination of the limit of plasma-arc welding speed, after reaching which there is no more significant increment in strength indices, as well as reducing the width of HAZ and deformation of the structure.

AIM AND TASKS OF RESEARCH

The aim of the work is to set reasonable limits for an increase in the speed of plasma-arc welding at a variable polarity asymmetrical current on the basis of determination of the effect of this parameter on the formation of welds, structure, change in mechanical properties of joints, distribution of temperature fields and stress-strain state of welded joints.

To achieve this aim, the following tasks were solved:

● determination of dependencies of formation, structure and change in mechanical properties of butt joints of alloys of the alloying systems Al–5Mg–Mn, Al–3Cu–1.8Li and Al–6Cu–Mn on the speed of plasma-arc welding at a variable polarity asymmetrical current;

● determination of distribution of temperature fields in welded plates from aluminium alloys, depending on the speed of plasma-arc welding;

Table 1. Chemical composition of aluminium alloys being welded, wt.%

Grade	Al	Cu	Mg	Mn	Zr	Ti	Zn	Fe	Si	Li
AMg5	Base	0.1	5.0	0.8	–	0.02		0.5	0.5	–
1201	–"–	6.0	–	0.4	–	0.06	0.2	0.4	0.4	–
1460	–"–	1.8	0.7	0.06	0.03	0.02	–	0.08	0.10	1.8

● investigation of residual deformation of welded joints produced by plasma-arc welding (by a constricted arc) at different welding speeds.

MATERIALS, EQUIPMENT AND RESEARCH METHODS

As welded specimens, aluminium alloys of alloying systems Al–Mg–Mn, Al–Cu–Mn and Al–Cu–Li with the thickness of sheets of 2.0 mm were considered (Table 1).

The studies were performed using a robotic complex PLAZER PAW-R for plasma-arc welding at a variable polarity asymmetrical current with the smart automatic system for control and monitoring of welding equipment (LLC "Scientific and Production Centre "PLAZER", Ukraine) (Figure 1). In addition to plasma-arc welding at a variable polarity asymmetrical current, the robotic complex allows performing a combined and hybrid welding with a combination of plasma-arc welding at a variable polarity with consumable electrode inert gas welding both without the formation of a common pool between two processes (combined welding), as well as with the formation of one common pool (hybrid welding).

PD-174M2 plasmatron designed at PWI (Figure 2, *a*, *b*) was used to carry out studies of weldability of selected aluminium alloys in wide ranges of a variable polarity asymmetrical current [13]. This plasmatron includes a set of replaceable plasma-forming nozzles

Figure 1. General appearance of the robotic complex of equipment PLAZER PAW-R for plasma-arc welding of lengthy welded joints at a variable polarity asymmetrical current with an up to 2000 mm extension of the robot hand and a system of the robot movement to 3000 mm (*a*, *b*) and a rack with power sources of the robot, plasmatron, cabinet with adaptation of commands for the robot and smart automatic system for monitoring of welding equipment (*c*): *1* — anthropomorphic welding robot; *2* — welding plasmatron; *3* — smart system for control of robotic welding process; *4* — plasma module; *5* — power source of plasma welding; *6* — welding table with an assembly and welding device; *7* — system for linear movement of robot on rails; *8* — double-axial rotator-manipulator; *9* — mechanism for filler wire feed
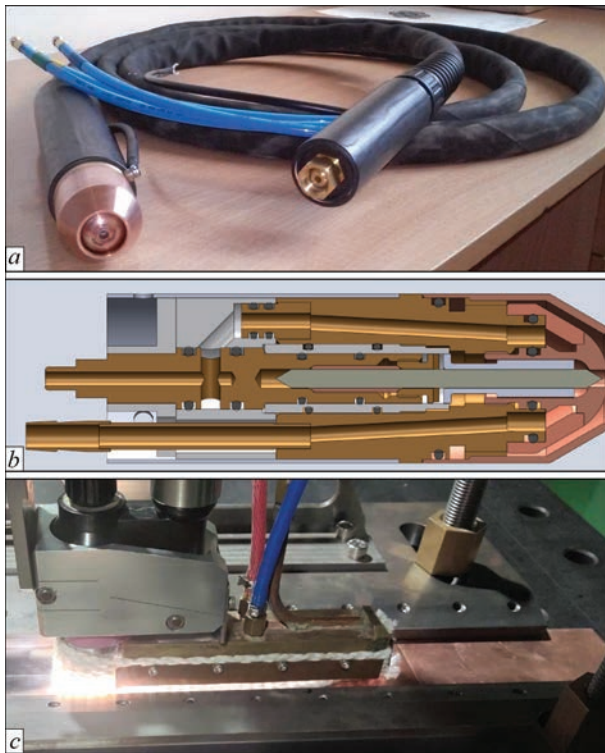
Figure 2. Appearance (*a*), cross-section of 3D-model (*b*) of welding plasmatron PD-174M2 for welding of aluminium alloys at a variable polarity asymmetrical current in the range from 80 to 350 A at DC 100 % and the process of robotic welding using an elongated gas protection nozzle (*c*)

with the holes of diameters from 2.0 to 4.5 mm with a step of 0.5 mm. For welding alloys with an increased fluidity of liquid metal, plasma-forming nozzles with 2 or 4 additional holes with a diameter of 1.0 mm are included in the set. The task of additional holes is to reduce the excessive gas pressure on the axis of a plasma-forming nozzle and to provide additional elongation of the plasma arc. Also, for the efficient operation of this plasmatron in the specified range of currents, there is an option of using tungsten electrodes with a diameter from 3.2 to 6.0 mm by replacing a collet

Figure 3. Appearance of welded joint of AMg5M alloy in the assembly and welding device immediately after plasma-arc welding at a variable polarity asymmetrical current at a speed of 200 cm/min

and a washer-current-lead for electrode unit, as well as a ceramic insulator-aligner, which is made of special thermal-resistant ceramics. For welding at high speeds (above 120 cm/min) using this plasmatron, a nozzle with elongated gas protection with a length of 200 mm and a width of 50 mm was used (Figure 2, *c*).

As a criterion "high-speed welding", an excess of speed of the base process of arc welding of high-strength aluminium alloys (with the strength higher than 300 MPa) by 2 or more times, TIG welding at a variable polarity current was chosen. A limiting factor in plasma-arc welding at a variable polarity asymmetrical current in our case were the technological capabilities of welding plasmatrons, namely the maximum current load of up to 325 A.

The maximum speeds of plasma-arc welding at a variable polarity asymmetrical current in the flat position on the substrate with a forming groove and the use of a filler wire are shown in Table 2. Figure 3 shows the outer appearance of welded joint of AMg5M alloy in the assembly and welding device immediately after the end of plasma-arc welding at a variable polarity asymmetrical current of 200 cm/min speed. In welding, the change in the indices of strength of the welded joint and weld metal were taken into account. The following alloys were considered: AMg5M (Al–5 % Mg–8 % Mn), which is thermally unstrengthened and should be little sensitive to the loss of strength in the HAZ, thermally strenghtened alloys 1201 (Al–6 % Cu–0.4 % Mn) and aluminium-lithium alloy 1460 (Al–3.0 % Cu–1.8 % Li). The base metal of 1201 and 1460 alloys tend to lose strength in the HAZ of the arc.

RESULTS OF STUDYING THE EFFECT OF SPEED OF PLASMA-ARC WELDING AT A VARIABLE POLARITY ASYMMETRICAL CURRENT

STUDYING THE EFFECT OF PLASMA WELDING SPEED ON WELDS FORMATION, THEIR STRUCTURE AND MECHANICAL PROPERTIES

An increase in the speed of plasma-arc welding of sheets of 1.8 mm thick 1201 alloy (Al–6Cu–Mn)

Table 2. Maximum welding speeds depending on thermophysical properties of aluminium alloys

Alloy	Thickness, mm	Maximum welding speed, cm/min
AMg5M (Al–5 % Mg–0.8 % Mn)	2.0	300
1201 (Al–6 % Cu–0.4 % Mn)	1.8	200
1460 (Al–3.0 % Cu–1.8 % Li)	2.0	300

from 30 to 300 cm/min causes a 40 % decrease in the amount of input energy (from 124 to 74 kJ/m), as well as a 33 % reduction in area of the base metal softening zone under the influence of heat action from the welding arc (Figure 4).

In welding at a high speed, dendrites are oriented clearly perpendicular to the weld axis, unlike the option with a low speed, where twisting of dendrites and their coupling along the weld axis at an acute angle is observed. Microstructure of welded joints of sheets of 1.8 mm thick from 1201 alloy produced by plasma-arc welding at a speed of 30 cm/min is shown in Figure 5.

In the weld metal of 1201 alloy of the alloying system Al–Cu–Mn produced by a constricted arc of a variable polarity asymmetrical current at a welding speed of 30 cm/min, the pores of up to 60 μm are observed. These pores are mainly localized on the boundaries of the fusion area with the base metal. In the weld metal dendrites are observed, the first-order axes of which are located mainly along the weld axis. On the boundaries of grains, coarse clusters of eutectic are observed. Zones of loosenings are encountered.

Microstructure of joints of sheets of 1201 alloy of 1.8 mm thick, produced by plasma-arc welding at a variable polarity current at a speed of 300 cm/min in the flat position on the substrate without using filler, is shown in Figure 6. The comparison of welds produced at a speed from 30 to 300 cm/min showed that with an increase in plasma-arc welding speed, the
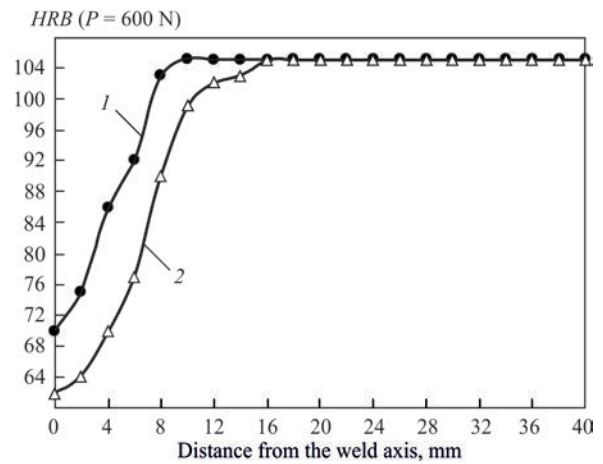

Figure 4. Distribution of hardness in the cross-sections of joints of sheets of 1201 (A1–Cu–Mn) alloy of 1.8 mm thick, produced by plasma-arc welding at a variable polarity current in the flat position at a speed of 30 and 300 cm/min; *1* — 18; *2* — 180 m/h

amount of pores in the weld metal increases, but their sizes decrease by 1.5–2.0 times.

In plasma-arc welding of sheets of 1.8 mm thick of 1201 alloy (Al–Cu–Mn) at a speed of 300 cm/min with the filler wire, the molten metal formed during melting of the wire, does not have time to mix with the molten metal of the welding pool. An excess of metal, which should form the upper bead of the weld, does not spread normally, the upper bead of the weld is formed unevenly and deep undercuts are formed along the boundary of the weld fusion zone with the base metal. The use of a filler in the form of an insert
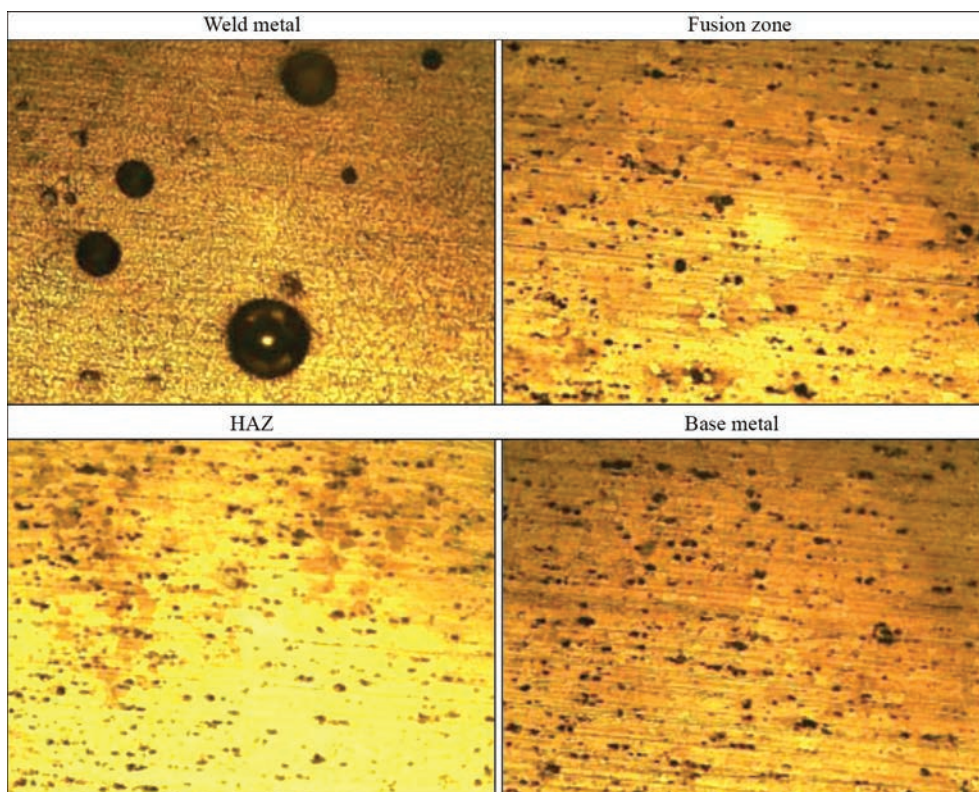

Figure 5. Microstructure (×150) of welded joint of sheets of 1.8 mm thick from 1201 (Al–6Cu–Mn) alloy produced by plasma-arc welding in the flat position without a filler at a speed of 30 cm/min
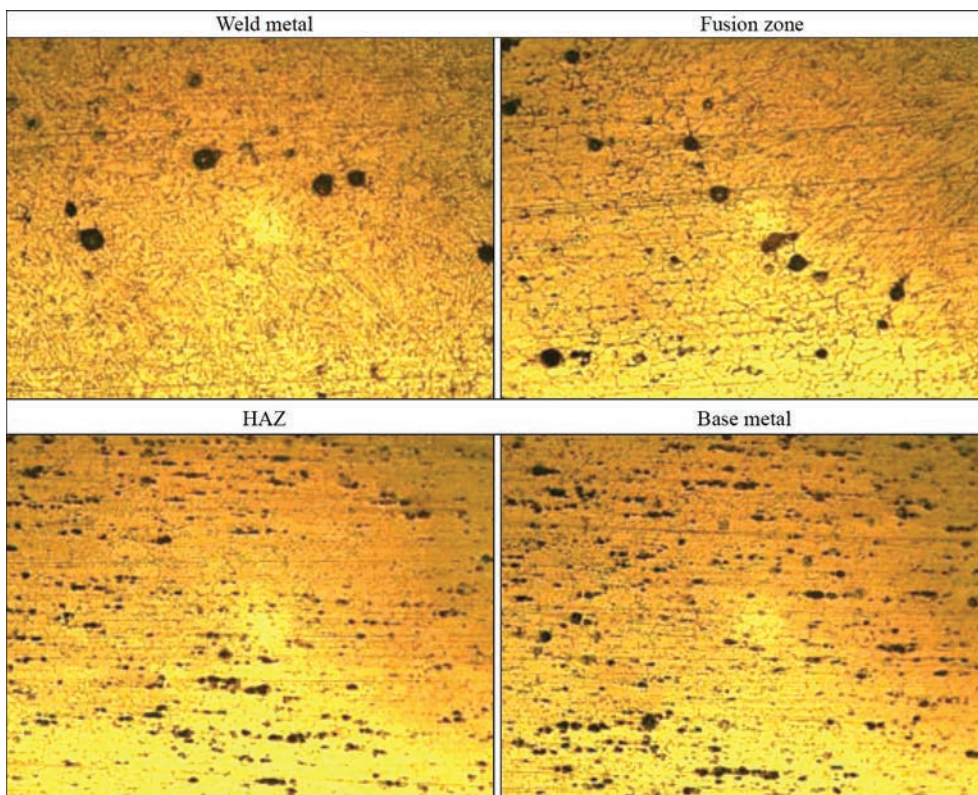
Figure 6. Microstructure (×150) of welded joint of sheets of 1.8 mm thick from 1201 (Al–Cu–Mn) alloy, produced by plasma-arc welding in the flat position without a filler at a speed of 300 cm/min

from a strip cut out from the base metal also does not provide the qualitative formation of the weld surface. The strip melts unevenly. Splashing of the molten metal under the influence of a plasma jet is observed. On the surface at the center of the weld, a chain of pores coming to the surface remains.

The presence of deep undercuts (up to 0.5 mm or more) and the presence of pores over the whole weld metal, produced at a speed of 300 cm/min, cause not too high strength of the welded joint (249–251 MPa). As the welding speed is reduced to 200 cm/min, a clearly expressed chain of surface pores disappears from the surface, as well as the conditions of formation of the transition from the weld to the base metal are improved. In this case, the strength of the weld-

Figure 7. Diagram of change in strength of welded joints depending on speed of welding sheets of 1.8 mm thick from 1201 (Al–Cu–Mn) alloy produced by plasma-arc welding at a variable polarity current: *1* — welded joint; *2* — weld metal

ed joint is 279–280 MPa, which exceeds the strength of the welded joint of 1201 alloy of 2.0 mm thick (246 MPa) produced by TIG welding at a speed of 20 cm/min (Figure 7).

The welds produced at a speed of 40 cm/min (24 m/h) have a cellular-dendritic structure typical of the cast state with the formation of a central crystallite. The structure of welds produced at speeds of 120 and 200 cm/min, is characterized by the absence of a central crystallite and a narrower region of columnar elongated small crystallites with a large number of cells and small equiaxial dendrites in the central part of the weld. An increase in crystallization rate at a welding speed of 120 cm/min provides the formation of branched dendrites of a solid solution and phases evenly located between them, which did not become a part of their composition, the shape and sizes of which are determined by the value of crystallization rate (Figure 8).

In the structure of welds produced at 120 cm/min, dendrites 3–4 times smaller are observed than in welding at a speed of 40 cm/min. The orientation of axes of the first-order dendrites is changed. Unlike welding at a low speed, these axes are directed perpendicularly to the longitudinal axis of the weld, which may be a consequence of not only high welding speed, but also a power concentration in the plasma jet and additional forced effect of plasma-forming gas.
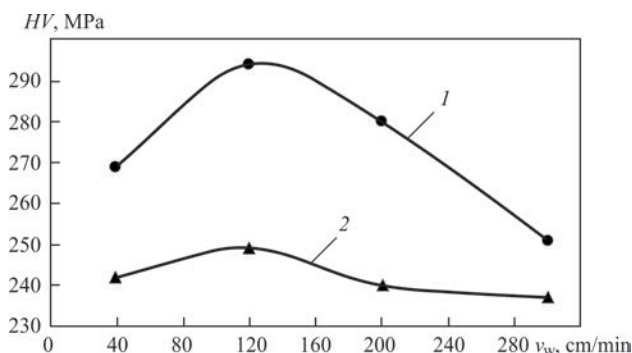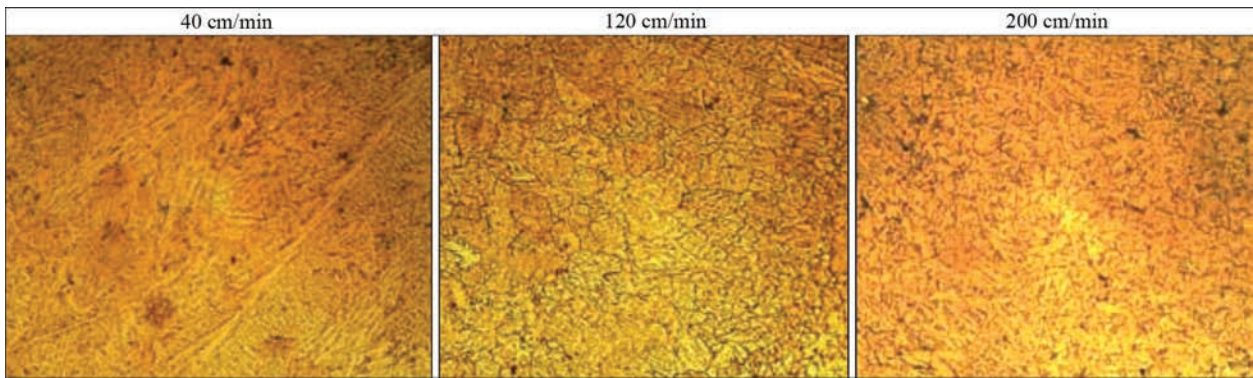
Figure 8. Microstructure (×150) of weld metal produced by plasma-arc welding of sheets of 1.8 mm thick from 1201 (Al–Cu–Mn) alloy by a variable polarity current at different welding speeds

A change in the strength indices at different welding speeds is also observed in plasma-arc welding of a thermally strengthened 1460 alloy, which contains Cu and Li. The introduction of 1.9–2.3 % Li into the chemical composition of 1460 alloy allowed reducing the specific weight of 1460 alloy compared to 1201 alloy and increase its strength to 574 MPa (compared to 439 MPa for 1201 alloy).

An increase in the interval of increment of strength indices and their smooth decrease at a speed of 300 cm/min may be explained by a higher fluidity of the liquid metal of 1460 alloy compared to 1201 alloy by introducing Li. The reduction in strength at a welding speed of 300 cm/min is predetermined by the start of undercuts formation and deterioration of conditions of weld degassing (Figure 9).

In 1460 alloy, the process of reduction in strength begins after an increase in the welding speed above 200 cm/min. As in 1201 alloy, the process of reduction in strength is also predetermined by the formation of undercuts along the fusion line and an increase in porosity in the weld metal.

In plasma-arc welding of a thermally unstrenghtened AMg5M (Al–Mg–Mn) alloy of 2.0 mm thick, also an increase in the growth of strength indices of welded joints with the growth of speed of plasma-arc welding is observed (Figure 10). However, unlike 1201 and 1460 alloys, which are thermally strengthened and more sensitive to heat input, in the mentioned alloy, the growth in strength indices occurs more slowly. At the same time, an increase in the welding speed above 200 cm/min, a decrease in the strength indices of the welded joint by the formation of undercuts in the fusion zone is observed. In this case, the size of undercuts is smaller compared to alloys containing Cu.

INFLUENCE OF PLASMA WELDING SPEED ON DISTRIBUTION OF TEMPERATURE FIELDS IN WELDED SPECIMENS

To calculate the regularities of temperature change, depending on the speed of plasma-arc welding, a procedure for calculating the temperature field in the plate at welding speeds of up to 20 cm/min (12 m/h) and from 30 to 300 cm/min (from 18 to 180 m/ h) was used [14]. The calculation was performed by the finite element method. For welding speeds of up to 20 cm/min, the calculation scheme was chosen using a point moving heating source, and for welding speeds above 30 cm/min — a powerful linear heating source.

The maximum temperatures were determined from the temperature distribution diagrams for welding at a speed of up to 20 cm/min (Figure 11) and diagrams
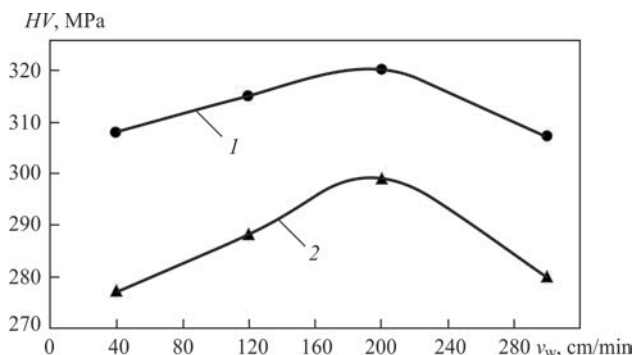

Figure 9. Diagram of change in strength of welded joints depending on speed of welding sheets of 2.0 mm thick from 1460 (Al–Cu–Li) alloy produced by plasma-arc welding at a variable polarity current: *1* — welded joint; *2* — weld metal
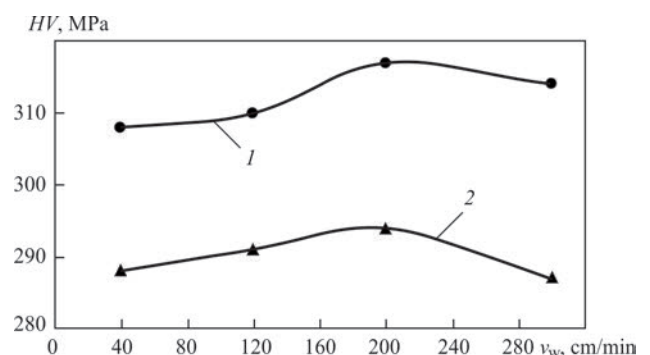

Figure 10. Diagram of change in strength of welded joints depending on speed of welding sheets of 2.0 mm thick from AMg5M (Al–Mg–Mn) alloy, produced by plasma-arc welding at a variable polarity current: *1* — welded joint; *2* — weld metal
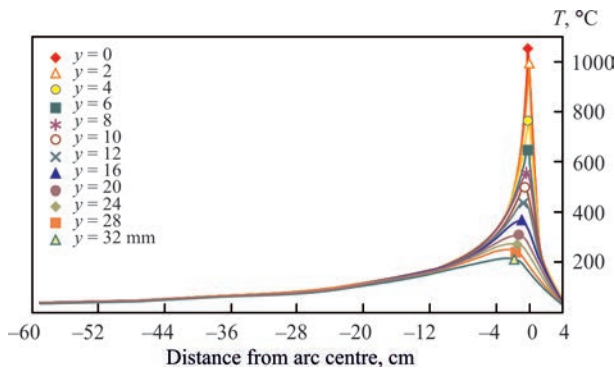
23

Figure 11. Diagram of temperature distribution in plasma-arc welding of aluminium 1201 (Al–Cu–Mn) alloy of 6.0 mm thick at a variable polarity current in the flat position at a speed of 20 cm/min (12 m/h)

of thermal cycles for the processes at a speed above 30 cm/min, for example, 200 cm/min (Figure 12).

Figures 13 and 14 show the diagrams of maximum temperatures in the cross-section of the welded joint obtained thanks to performed calculations.

When analyzing the diagrams of distribution of maximum temperatures (Figures 13, 14) in plasma-arc welding of sheets of 1.8 mm thick from 1201 alloy at a variable polarity asymmetrical current and welding speeds from 40 to 300 cm/min, it was found that at the same step between the speeds of 80 cm/min, the difference in the temperature between the curves of the distribution of maximum temperatures depends on the range of speeds changes (in the range from 40 to 120 cm/min, the differences in the temperature between the points at a distance of 5 mm from the weld axis are 3–4 times higher than in the speed range from 120 to 200 cm/min).

At a distance of more than 4 mm from the axis, in plasma-arc welding of aluminium 1201 alloy of 1.8 mm thick at a variable polarity asymmetrical current with a change in welding speed from 120 to 180 cm/min, the temperature changes on average by 50 °C, which does not significantly affect both the change of
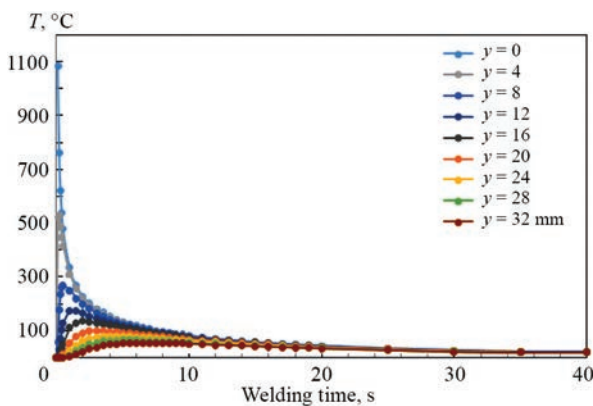

Figure 13. Distribution of maximum temperatures occurring in the sheets of 1201 alloy of 1.8 mm thick joined by plasma-arc welding at a variable polarity current at welding speeds of 40 (curve *1*) and 120 cm/min (curve *2*)

hardness, as well as the change of mechanical properties of welded joints.

STRESS-STRAIN STATE IN WELDED JOINTS PRODUCED BY WELDING USING CONSTRICTED ARC AT DIFFERENT WELDING SPEEDS

In order to improve the influence of plasma-arc welding speed on the obtained results, a study of a stress-strain state was conducted according to the procedure described in [15], making the necessary calculations with the use of the MatCAD software. The calculation was carried out on several indices of stress-strain state of plane specimens after welding. The calculations took into account the thickness of welded plates and their thermophysical and mechanical properties.

Figure 15 shows the features of changing the width of the plastic deformation zone depending on the speed of plasma-arc welding of aluminium alloys of specimens of 2.0 mm thick from AMg5M (Al–Mg–Mn) alloy and specimens of 1.8 mm thick from 1201 (Al–Cu–Mn) alloy at a variable polarity asymmetrical current. A similar regularity is observed for other indices, such as longitudinal reduction in area of the spec-

Figure 12. Thermal cycle in plasma-arc welding of sheets of 1.8 mm thick from 1201 (Al–Cu–Mn) alloy at a variable polarity current and a speed of 200 cm/min (120 m/h)
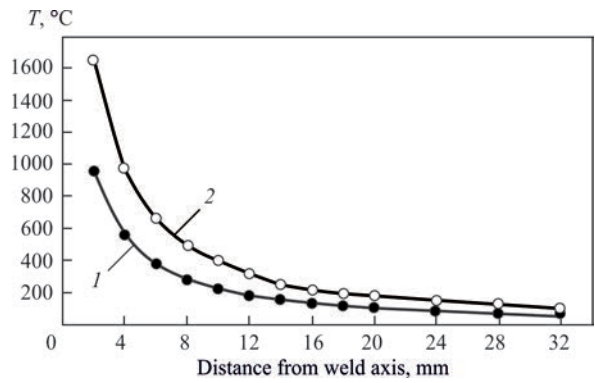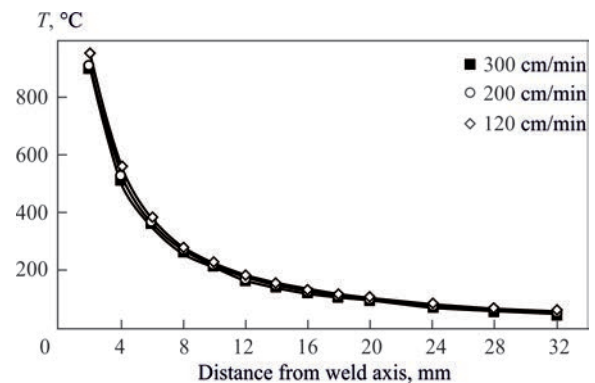

Figure 14. Distribution of maximum temperatures occurring in the sheets of 1201 alloy of 1.8 mm thick joined by plasma-arc welding at a variable polarity current at welding speeds from 120 to 300 cm/min
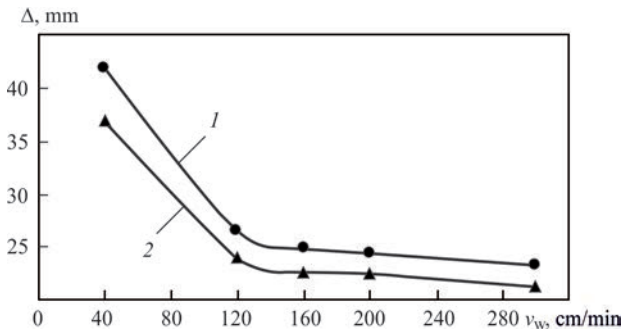
Figure 15. Change in the width of plastic deformation zone in welded specimens of 1.8–2.0 mm thick of AMg5M (Al–Mg–Mn) and 1201 (Al–Cu–Mn) alloys depending on speed of plasma-arc welding: *1* — Al–6Cu–Mn; *2* — Al–5Mg–Mn
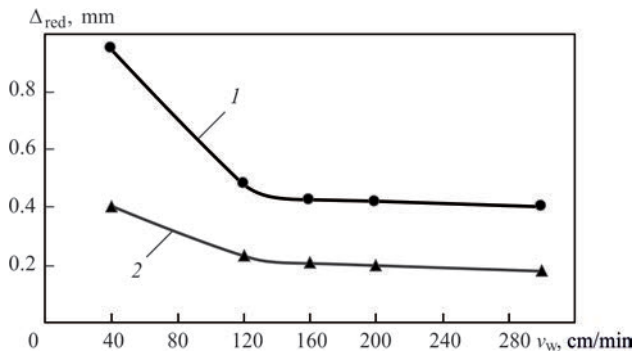

Figure 16. Change in the longitudinal reduction in area of the specimen of 1.8–2.0 mm thick of AMg5M (Al–Mg–Mn) and 1201 (Al–Cu–Mn) alloys depending on speed of plasma-arc welding: *1* — Al–6Cu–Mn; *2* — Al–5Mg–Mn
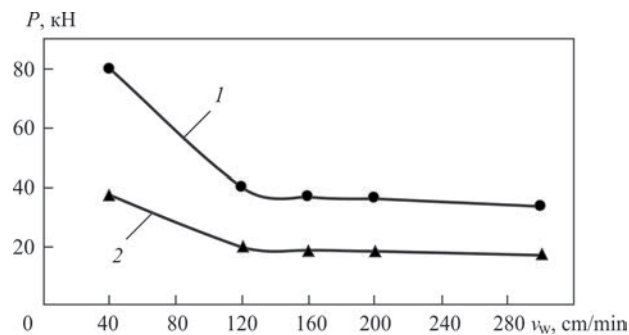

Figure 17. Change in the upsetting force of the specimen weld of 1.8–2.0 mm of AMg5M (Al–Mg–Mn) and 1201 (Al–Cu–Mn) alloys depending on speed of plasma-arc welding: *1* — Al–6Cu–Mn; *2* —Al–5Mg–Mn

Figure 18. Change in the width of plastic deformation zone in welded specimens of 4.0 mm thick of AMg5M (A1–Mg–Mn) alloy depending on speed of plasma-arc welding

Figure 19. Change in the longitudinal reduction in area of the specimen of 4.0 mm thick of AMg5M (A1–Mg–Mn) alloy depending on speed of plasma-arc welding

Figure 20. Change in the weld upsetting force of the specimen of 4.0 mm thick from AMg5M (Al–Mg–Mn) alloy depending on speed of plasma-arc welding

imen (Figure 16) and the weld upsetting force during welding (Figure 17).

A more pronounced tendency of exponential decrease in the intensity of indices of stress-strain state with an increase in welding speed is observed in plasma-arc welding of specimens of 4.0 mm thick (Figures 18–20). As is seen from the abovementioned diagrams, there is a certain speed, after which the further increase in welding speed does not lead to a decrease in residual deformations and stresses in the studied alloys.

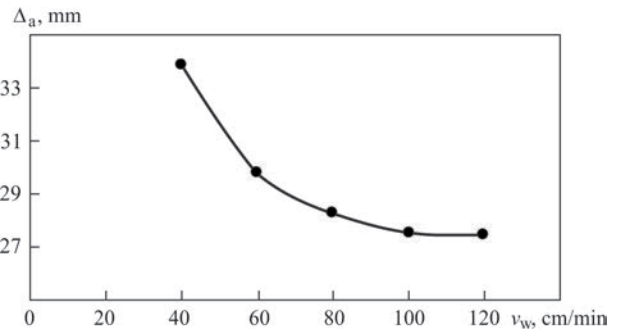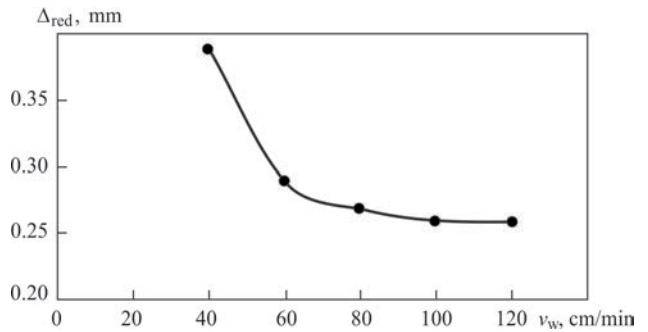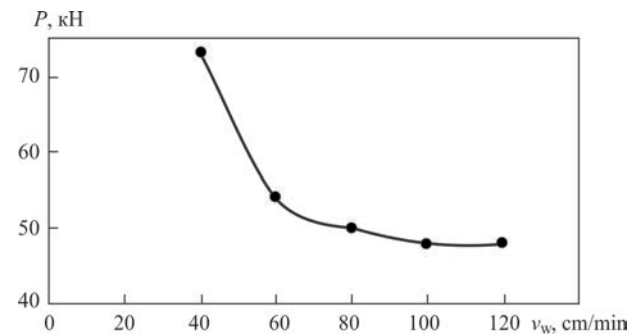The regularity of rapid reduction in indices of stress-strain state in the specimens after welding is observed also in plasma-arc welding of sheets of Al–Mg–Mn alloying system in two delivery states of this AMg6M and AMg6N alloy. The alloys have a similar chemical composition, but differ in strength indices of the base metal and yield strength (Figures 21, 22). In AMg6N alloy due to plastic deformation (peening), the indices of strength and yield strength were increased compared to AMg6M alloy. Taking into account the similar chemical composition of alloys, plasma-arc welding was performed at the same modes of current, balance of variable polarity current, frequencies of variable polarity current and flow rate of plasma-forming gas.

Analyzing the regularities of change in the indices of stress-strain state in plasma-arc welding, it can be
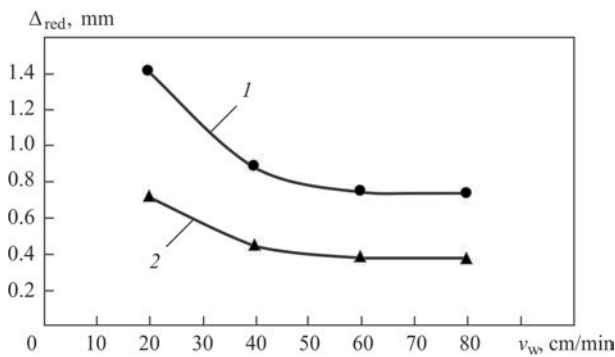
Figure 21. Change in the longitudinal reduction in area of 6.0 mm thick specimen of AMg6M (*1*) and AMg6N (*2*) alloys depending on speed of plasma-arc welding

concluded that welding speed, at which a rapid decrease in the indices of stress-strain state ends and changes begin by 1–2 %, first of all depends on the thickness of welded metal. Figure 23 shows a diagram of dependence of such speed on thickness of aluminium alloys.

DISCUSSION OF RESULTS OF STUDYING INFLUENCE OF TECHNOLOGICAL METHODS ON THE PECULIARITIES OF STRUCTURE FORMATION

According to metallographic analysis, the structure of the weld of 1201 alloy represents a solid solution with fine-dispersed $CuA1_2$ phase inclusions and eutectics of type $(\alpha + CuA1_2)$. The inclusions of oxide films and microcracks are not observed, but in the places of location of precipitates of excessive phases, separate micropores of less than 0.1 μm and microloosenings are encountered, the number and nature of whose location depends on the welding speed and crystallization rate.

The weld structure of 1201 alloy produced by plasma-arc welding at a speed of 40 cm/min contains crystallites differing in shape and direction. Near the fusion boundary, where the first stage of crystallization occurs, the structure is mostly fine crystalline. The processes of heat removal and crystallization overcooling occurring in the welding pool during cooling
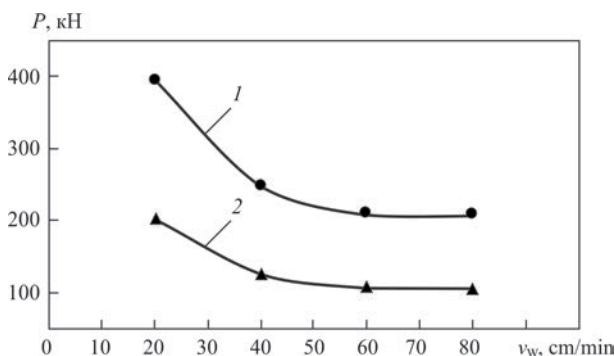

Figure 22. Change in the upsetting force of the specimen of 6.0 mm thick of AMg6M (*1*) and AMg6N (*2*) alloys depending on speed of plasma-arc welding
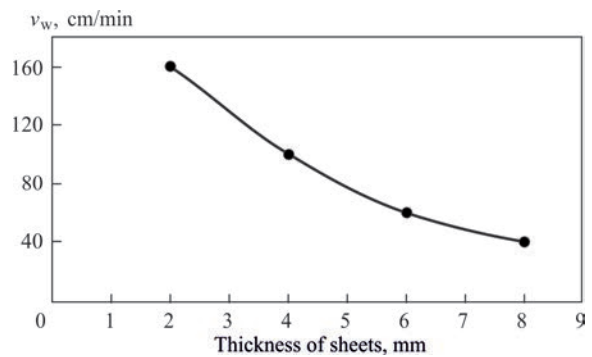

Figure 23. Dependence of welding speed on thickness of welded metal, at which a decrease in the indices of stress-strain state in welded specimens of aluminium alloys ends

of the metal and its crystallization, contribute to the formation of the columnar crystallites zone, which are oriented mainly to the vector of melting isotherm. In the centre of the weld, a central crystallite is observed, whose boundary is adjacent to the side crystallites. As the welding speed increases to 120 and 200 cm/min, the formation of central crystallite is not observed.

The microstructure of the welds of 1201 alloy with an increase in welding speed from 40 to 120 cm/min is featured by a decrease in the sizes of dendrites from 10–40 to 3–14 μm and a number of intermediate phases θ′ ($CuA1_2$) and S′ ($A1_2CuMg$) at a constant amount resistant to the thermal effect of the phase θ′ ($CuA1_2$). An even greater tendency to reduce the sizes and number of mentioned phases is observed in the structure of welds produced at a speed of 200 cm/min.

The similar tendencies of structure formation are observed in welding of other studied alloys. The reduction in crystallization stage, at which phase embryos and a period of dendrites entanglement arises and develops, helps to increase the volume of solid solution, which can be the basis for increasing the strength of the weld metal. The gaps between the branches of dendrites are filled with liquid metal, the interfacial boundaries are stabilized. As a result, the solid phase becomes cellular and the sizes of crystallites in the welds decrease by about 3 times.

When welding speed 5 times increases (from 40 to 200 cm/min), the transformation processes occur more intensively, which causes the transition of microstructure of welds to a dendritic structure with a high density and dispersion of particles precipitates and strengthening phases. This is predetermined by the change in the size of the temperature gradient on the interface of the solid solution of liquid metal and phases, the rate of growth and distribution of the solution at the interfacial boundary of their growth (along the crystallization front).

Metallographic and microdurometric examinations showed that at a high welding speed (300 cm/min), dendrites are formed which are 3–4 times smaller than

at a welding speed of 30 cm/min. The orientation of the first-order dendrites is changed. Unlike welding at 30 cm/min, these axes of dendrites are directed perpendicular to the longitudinal axis of the weld. Refinement of dendrites may explain an increase in the microhardness of the weld (for example, by 5–25 % for 1201 alloy), produced at a speed of 300 cm/min, compared to the weld produced at a speed of 30 cm/min (Figure 4).

It was found that with an increase in the welding speed from 30 (Figure 5) to 300 cm/min (Figure 6), an increase in the number of pores with a decrease in their size (approximately by 1.5–2.0 times) occurs. This phenomenon may be explained by the fact that due to a higher welding speed, the pores did not have time to grow to large sizes, and a short time of existence of the pool in the liquid state deteriorates the conditions of weld degassing. The pores are localized mainly along the fusion zone of the weld with the base metal.

Mechanical tests showed a decrease in the strength of welded joints of aluminium alloys at an increase in the welding speed from 200 to 300 cm/min (Figures 7, 9, 10, 11). This is explained by the deterioration of the formation of the transition from the weld to the base metal and the formation of undercuts, as well as the formation of a chain of surface pores on the axis of the joint due to deterioration of the conditions of weld metal degassing. In the case of plasma-arc welding of AMg5M (Al–Mg–Mn) alloy at a variable polarity current (Figure 7), the effect of reducing the strength at an increase in the speed from 200 to 300 cm/min is not expressed so explicitly as for 1201 (Al–Cu–Mn) (Figure 4) and 1460 (Al–Cu–Li) alloys (Figure 6). This is caused by the fact that unlike 1201 and 1460 alloys, AMg5M alloy is not thermally strengthened, as well as the size of undercuts is smaller in the joints of AMg5M alloy compared to alloys containing Cu. It should be noted that in general the strength of plasma-arc welding of aluminium alloys is higher than the strength of TIG of these alloys. This is associated with an increase in the heat input in TIG, which leads to an increase in the sizes of dendrites and HAZ.

It was found that when the amount of copper in the composition of aluminium 1460 alloy (Al–3 % Cu–1.8 % Li) decreases, the speed of plasma-arc welding has a smaller effect on the change of the strength of welded joint (4–5%), a somewhat higher degree of copper on the strength of the weld metal (increases by 7 %) is observed at an increase in the welding speed from 40 to 200 cm/min. The further increase in speed leads to a decrease in strength indices, which is predetermined by the start of undercuts formation and deterioration of weld metal degassing.

Analysis of change in the temperature fields distribution in plasma-arc welding of 1201 alloy of 1.8 mm thickness showed a gradual decrease in HAZ size when welding speeds are changed from 40 to 120 cm/min and stabilization of this parameter with an increase in welding speed from 120 to 300 cm/min.

The studies of indices of stress-strain state in plasma-arc welding of specimens of the considered alloys showed that with an increase in speed, a tendency of almost exponential decrease in the value of these indices is observed (Figures 12–19). As is seen from the abovementioned diagrams, there is a certain speed (for example, 100 cm/min for the case of AMg5M alloy (Figures 15–17), after which the further increase in welding speed does not lead to a decrease in residual deformations and stresses in the studied alloys. Such speed depends not only on the grade of alloy, but also on its thickness (Figure 20).

CONCLUSIONS

1. A tendency of at least 2–3 times reduction in the sizes of dendrites and a change in the orientation of axes of the first-order dendrites to the orientation of the perpendicularly longitudinal axis of the weld at an increase in the speed of welding high-strength aluminium alloys of Al–5Mg–Mn, Al–3Cu–1.8Li and Al–6Cu–Mn alloying systems from 40 to 120 cm/min was revealed. The effect of an increase in the indices of strength of welded joints reaching the welding speed extremum in the range of 120–200 cm/min with their subsequent decline caused by deterioration of the conditions of a welded joint formation due to the formation of undercuts and an increase of pores in the weld metal was determined. It is shown, that for aluminium Al–6Cu–Mn and Al–3Cu–1.8Li alloys, which are thermally strengthened, a rapid increase in the indices of strength is observed when the welding speed extremum is reached. Here, a decrease in the amount of copper in the base metal from 6.0 to 3.0 % allows increasing the index of welding speed extremum from 120 to 200 cm/min.

2. It was found that as the speed of plasma-arc welding of sheets of 1.8 mm thick from the Al–Cu–Mn alloy at a variable polarity asymmetrical current grows from 40 to 120 cm/min, the maximum temperature at a distance of 5 mm from the weld axis decreases from 850 to 450 °C. The further increase in the welding speed to 200 and 300 cm/min leads to a decrease in the maximum temperature at this point to 425 and 400 °C, respectively. Therefore, a decrease in the intensity of falling temperature at a point 5 mm from the weld axis with the growth of welding speed above 120 cm/min is observed.

3. It is shown that the value of residual deformations sharply decrease by 2 times when a certain welding speed extremum is achieved in the range of 120–200 cm/min, and the further growth in the welding speed does not cause a significant decrease in residual deformations, i.e. the change in the deformation value is not more than 5 %. On the example of Al–Mg–Mn alloy it is shown that such regularities are also typical not only for 2.0 mm thickness, but also observed in welding of specimens with the thickness range of 4–8 mm. This allows using these results to predict indices of strength and stress-strain state of welded joint, as well as weld metal for these thicknesses with an increase in the speed of plasma-arc welding at a variable polarity asymmetrical current higher than the "peak" value.

REFERENCES

1. Guan, R., Lou, H., Huang, H. et al. (2020) Development of aluminium alloy materials: Current status, trend, and prospects. *Strategic Study of Chinese Academy of Engineering*, 22(**5**), 68–75. DOI: https://doi.org/10.15302/J-SSCAE-2020.05.013

2. Samiuddin, M., Li, J.-L., Taimoor, M. et al. (2021) Investigation on the process parameters of TIG-welded aluminium alloy through mechanical and microstructural characterization. *Defence Technology*, 17(**4**), 1234–1248. DOI: https://doi.org/10.1016/j.dt.2020.06.012

3. Lis, A., Mogami, H., Matsuda, T. et al. (2018) Hardening and softening effects in aluminium alloys during high-frequency linear friction welding. *J. Materials Proc. Technology*, **255**, 547–558. DOI: https://doi.org/10.1016/j.jmatprotec.2018.01.002

4. Xu, B., Chen, S., Jiang, F. et al. (2019) The influence mechanism of variable polarity plasma arc pressure on flat keyhole welding stability. *J. of Manufacturing Processes*, **37**, 519–528. DOI: https://doi.org/10.1016/j.jmapro.2018.12.026

5. Xu, B., Tashiro, S., Jiang, F. et al. (2019) Effect of arc pressure on the digging process in variable polarity plasma arc welding of A5052P aluminium alloy. *Materials*, **12**, 1071, 1–17. DOI: https://doi.org/ 10.3390/ma12071071

6. Lang, R., Han, Y., Bai, X., Hong, H. (2020) Prediction of the weld pool stability by material flow behavior of the perforated weld pool. *Materials*, 303(**13**), 1–20. DOI: https://doi.org/10.3390/ma13020303

7. Klett, J., Bongartz, B., Wolf, T. et al. (2023) Plasma welding of aluminium in an oxygen-free argon atmosphere. *Advances in Materials Sci.*, 23, 75(**1**), 5–18. DOI: https://doi.org/10.2478/adms-2023-0001

8. Labur, T.M., Grinyuk, A.A., Poklyatsky, A.G. (2006) Mechanical properties of plasma welded joints on aluminium-lithium alloys. *The Paton Welding J.*, **6**, 32–34.

9. *Selva* Bharathi, R., Siva Shanmugam, N., Murali Kannan, R., Arungalai Vendan, S. (2018) Studies on the parametric effects of plasma arc welding of 2205 duplex stainless steel. *High Temperature Materials and Processes*, 37(**3**), 219–232. DOI: https://doi.org/10.1515/htmp-2016-0087

10. Sathishkumar, M., Manikandan, M., Subramani, P. et al. (2020) Effect of welding speed on aspect ratio of hastelloy X weldment by keyhole plasma arc welding (K-PAW). *Materials Today*, 22(**4**), 3297–3304. DOI: https://doi.org/10.1016/j.matpr.2020.03.291

11. Batool, S., Khan, M., Jaffery, S. et al. (2015) Analysis of weld characteristics of micro-plasma arc welding and tungsten inert gas welding of thin stainless steel (304L) sheet. Proceedings of the Institution of Mechanical Engineers, Pt L: *J. of Materials: Design and Applications*, 230(**6**). DOI: https://doi.org/10.1177/1464420715592

12. Korzhyk, V., Khaskin, V., Grynyuk, A. et al. (2022) Comparison of the features of the formation of joints of aluminium alloy 7075 (Al–Zn–Mg–Cu) by laser, microplasma, and laser-microplasma welding. *Eastern-European J. of Enterprise Technologies*, 115 (**1–12**), 38–47. DOI: https://doi.org/10.15587/1729-4061.2022.253378

13. Grinyuk, A.A., Korzhyk, V.N., Babich, A.A. et al. (2016) Unified plasmatron for consumable electrode constricted arc welding. *Tekhnologicheskie Sistemy*, **4**, 86–89 [in Russian].

14. Lobanov, L.M., Pashchyn, M.O., Mikhodui, O.L. et al. (2021) Modeling of stress-strain states of AMg6 alloy due to impact action of electrode-indenter in electrodynamic treatment. *The Paton Welding J.*, **6**, 2–11. DOI: https://doi.org/10.37434/tpwj2021.06.01

15. (2018) *Physical processes in welding and treatment of materials. Theoretical studies, mathematical modeling, computing experiment*: Collect. of articles and reports. Ed. by I.V. Krivtsun. Kyiv, IAW [in Russian].

ORCID

V.M. Korzhyk: 0000-0001-9106-8593
A.A. Grynyuk: 0000-0002-6088-7980,
V.Yu. Khaskin: 0000-0003-3072-6761
E.V. Illyashenko: 0000-0001-9876-0320,
S.I. Peleshenko: 0000-0001-6828-2110,
A.O. Aloshyn: 0000-0001-9696-6800,
I.O. Skachkov: 0000-0001-6933-1148
O.V. Dolyanivska: 0000-0001-8396-2894

CONFLICT OF INTEREST

The Authors declare no conflict of interest

CORRESPONDING AUTHOR

V.M. Korzhyk
E.O. Paton Electric Welding Institute of the NASU
11 Kazymyr Malevych Str., 03150, Kyiv, Ukraine.
E-mail: vnkorzhyk@gmail.com

JOURNAL HOME PAGE

https://patonpublishinghouse.com/eng/journals/tpwj